ELSEVIER

Journal of Organometallic Chemistry 634 (2001) 185–192

Journal of Organometallic Chemistry

www.elsevier.com/locate/jorganchem

Continuous wave and pulse EPR as a tool for the characterization of monocyclopentadienyl Ti(III) catalysts

Sabine Van Doorslaer [a], Johan J. Shane [a], Stefan Stoll [a], Arthur Schweiger [a,*], Mirko Kranenburg [b], Robert J. Meier [b]

[a] *Physical Chemistry, ETH–Zurich, CH-8093 Zurich, Switzerland*
[b] *DSM Research BV, P.O. Box 18, 6160 MD Geleen, Netherlands*

Received 11 June 2001; accepted 31 July 2001

Abstract

Monocyclopentadienyl Ti(III) catalysts in which the cyclopentadienyl ring has a heteroatom-functionalized side chain are used in the polymerization of olefins and the co-polymerization of ethylene with propylene, 1-hexene, 1-octene and styrene. In this work, we show that a combined continuous wave and pulse EPR study of such complexes can reveal structural information where other analytical methods fail. Hyperfine sublevel correlation (HYSCORE) spectroscopy is found to be a powerful method to identify the type of nuclei surrounding the Ti^{3+} ion. For the first time, the hyperfine and nuclear quadrupole data of Ti(III)-bound ^{14}N nuclei are reported. The observed values are compared to known data of different transition metal complexes. Furthermore, the observed proton and lithium interactions are discussed. © 2001 Published by Elsevier Science B.V.

Keywords: Pulse EPR; Titanium complexes; Amino binding to titanium

1. Introduction

In the past years, there have been numerous investigations into the use of Group 4 organometallic complexes as homogeneous catalysts for polymerization of olefins [1]. Metallocenes of the type Cp'_2MR_2 and Cp'_2MX_2 (M = Ti, Zr, Hf; R = alkyl; Cp′ = substituted cyclopentadienyl; X = F, Cl) have been very successfully used as precursor compounds [2]. Upon reaction with a Lewis acid co-catalyst, such as $B(C_6F_5)_3$ or methylalumoxane (MAO), they give the cationic species $[Cp'_2MR]^+$ or $[Cp'_2MX]^+$ which are believed to be the actual catalysts. Monocyclopentadienyl precursors of the type $Cp'TiR_3$ have also been used to polymerize a wide range of olefins [3]. Special attention has been devoted to the synthesis of amido-functionalized cyclopentadienyl complexes of Group 4 metals [4]. Constrained-geometry compounds of the type (η^5-$C_5H_4SiR_2NR'$)TiMe (R, R′ = alkyl, aryl), in which η^5 coordination of the η^5-$C_5H_4SiR_2NR'$ ligand is reinforced by the simultaneous coordination of the amide nitrogen atom to the titanium ion, are found to be good catalysts for the polymerization of ethylene and 1-octene [4a,b]. Recently, there has also been an increasing interest in the use of P-functionalized alkyl or silyl side chains [4f,g,5].

The structure of newly designed catalysts is usually obtained from X-ray and/or NMR analyses. In the case of paramagnetic catalysts, the interpretation of the NMR spectra may become very difficult due to the presence of the unpaired electron(s). If additionally, single crystals cannot be grown or if structural information is needed about the catalyst in the solvent rather than in its crystalline form, alternative analytical methods have to be used.

Catalytically active organotitanium complexes have been reported to appear either in the Ti(IV) or in the Ti(III) form [1–5]. In contrast to the diamagnetic Ti(IV) complexes, paramagnetic Ti(III) catalysts give rise to an EPR (electron paramagnetic resonance) spectrum. Accordingly, continuous wave (CW) EPR has been extensively used to identify titanocenes [6], Ti(III) half-sandwich complexes [4a,5,7] and other Ti(III) cata-

* Corresponding author. Tel.: +41-1-632-4362; fax: +41-1-632-1021.
E-mail address: schweiger@esr.phys.chem.ethz.ch (A. Schweiger).

0022-328X/01/$ - see front matter © 2001 Published by Elsevier Science B.V.
PII: S0022-328X(01)01160-3

lysts [8]. In the past decades, different electron nuclear double resonance (ENDOR) and electron spin echo envelope modulation (ESEEM) techniques have been developed from which additional information on paramagnetic systems can be obtained [9]. Although these techniques have been applied extensively in different fields, they have found only limited applications in the area of Ti(III) catalysts. A few titanocenes have been studied using CW ENDOR [6b,10], and ESEEM has, to our knowledge, only been applied in the investigation of Ti(III)-containing zeolites [8c,e,f].

In this work, we show that pulse EPR methods can be applied to gain structural information on monocyclopentadienyl Ti(III) complexes where other analytical techniques fail. The CW EPR and hyperfine sublevel correlation (HYSCORE) spectra of [1-{2-(*t*-butyl)-2-sila-2,2-dimethyl}-2,3,4,5-tetramethylcyclopentadienyl]-methyl titanium(III), (η^5-$C_5Me_4SiMe_2N^tBu$)TiMe (**1**) (DOW Chemicals) are compared to those of [1-(dimethylaminoethyl)-2,3,4,5-tetramethylcyclopentadienyl]dimethyl titanium(III), ($C_5Me_4(CH_2)_2NMe_2$)-$TiMe_2$ (**2**), synthesized at DSM Research BV. The Ti(III) catalyst precursor **1** has a known structure, whereas no X-ray or NMR data are available for **2**. From a catalytic mechanistic point of view, the question whether the amino nitrogen is binding to Ti(III) in **2** is very important. It is shown that information on the nitrogen-binding can be obtained using the HYSCORE technique. In addition, the potential of this EPR method for the full characterization of Ti(III) catalysts is investigated.

2. Experimental

2.1. Chemicals

The synthesis of (η^5-$C_5Me_4SiMe_2N^tBu$)TiMe (**1**) was accomplished as described in [4b]. The synthesis of the half-sandwich cyclopentadienyl titanium complex ($C_5Me_4(CH_2)_2NMe_2$)$TiMe_2$ (**2**) was carried out on basis of the procedure described previously [4f,g,h].

2.2. Spectroscopy

The CW EPR spectra were recorded on a Bruker ESP300 spectrometer (microwave frequency 9.43 GHz), equipped with a N_2 gas flow cryostat. A microwave power of 1 mW, a modulation amplitude of 0.5 mT and a modulation frequency of 100 kHz were used. The X-band pulse EPR spectra (measured at 15 K throughout) were recorded on a Bruker ESP380 spectrometer (9.72 GHz) equipped with a liquid He flow cryostat from Oxford Instruments. The magnetic field was measured with a Bruker 035M NMR gaussmeter. In all pulse EPR measurements, a repetition rate of 1 kHz was used.

The HYSCORE experiments [11] were carried out with the pulse sequence $\pi/2-\tau-\pi/2-t_1-\pi-t_2-\pi/2-\tau-echo$ with pulse lengths $t_{\pi/2}=24$ and $t_\pi=16$ ns. The time intervals t_1 and t_2 were varied from 96 to 8272 ns in steps of 16 ns. Two spectra with $\tau=96$ and $\tau=176$ ns were recorded (blindspot removal). An eight-step phase cycle was used to eliminate unwanted echo contributions.

2.3. Theoretical background

EPR is based on the interaction of the magnetic moments of unpaired electrons with an external magnetic field $\mathbf{B}_0$ and internal fields exerted by magnetic nuclei in the vicinity of the electrons. In the case of Ti(III) complexes (electronic configuration $3d^1$), the dominating interactions are the electron Zeeman interaction (characterized by the **g** matrix) and the hyperfine interactions of the unpaired electron with the isotopes ^{47}Ti ($I=5/2$, natural abundance 7.75%) and ^{49}Ti ($I=7/2$, natural abundance 5.51%). Information on these interactions can be derived from the CW EPR spectrum. Pulse EPR methods, like HYSCORE, allow the identification and investigation of the hyperfine and nuclear quadrupole interactions of the magnetic ligand nuclei (e.g. ^{1}H, ^{14}N, ^{13}C, …). HYSCORE spectroscopy [9d,11] is a two-dimensional (2D) experiment in which a mixing π pulse creates correlations between the nuclear frequencies in two different electron spin (m_S) manifolds.

For a system with an unpaired electron ($S=1/2$) interacting with a nucleus with spin $I=1/2$ (e.g. ^{1}H), the spin Hamiltonian can be described in terms of the **g** matrix and the hyperfine matrix **A**. In general, the hyperfine matrix elements are the sum of an isotropic hyperfine coupling, a_{iso}, and a point–dipolar contribution, which depends on the distance r between the unpaired electron and the nucleus

$$A_{ij}=a_{iso}\delta_{ij}+(\mu_0/4\pi h)(g_n\beta_e\beta_n g_i(3l_i l_j-\delta_{ij})/r^3) \quad (i,j=x,y,z) \tag{1}$$

In case of an axial **g** matrix, $g_x=g_y=g_\perp$, $g_z=g_\parallel$, $l_x=\sin\beta$, $l_y=0$ and $l_z=\cos\beta$ where β is the angle between the $\mathbf{g}_\parallel$ axis and **r**. For an $S=1/2$, $I=1/2$ system, the nuclear frequencies in the two m_S manifolds are given by

$$\nu_{\alpha(\beta)}=[(A/2\pm\nu_I)^2+(B/2)^2]^{1/2} \tag{2}$$

with the nuclear Zeeman frequency $\nu_I=-g_n\beta_n B_0/h$. A and B describe the secular and pseudosecular part of the hyperfine coupling and are related to a_{iso} and r [9e]. In the HYSCORE experiment, the correlations between the nuclear frequencies lead to the cross-peaks (ν_α, ν_β)

and (ν_β, ν_α) in the 2D plot. The interpretation of HYSCORE spectra of disordered $S = 1/2$, $I = 1/2$ systems has been discussed by several authors [12,13].

The spin Hamiltonian of an $S = 1/2$, $I = 1$ system (e.g. one unpaired electron interacting with one ^{14}N nucleus) can be described in terms of the **g** matrix, the hyperfine matrix **A** and the nuclear quadrupole tensor **Q**. The principal values Q_x, Q_y and Q_z of the traceless **Q** tensor are usually expressed in terms of the quadrupole coupling constant e^2qQ/h and the asymmetry parameter η, with $Q_x = -(e^2qQ/4h)(1-\eta)$, $Q_y = -(e^2qQ/4h)(1+\eta)$ and $Q_z = e^2qQ/2h$. The HYSCORE spectra of an $S = 1/2$, $I = 1$ system are dominated by the cross-peaks between the double-quantum (DQ) frequencies [14]

$$\nu_{\alpha\beta}^{DQ} = 2[(a/2 \pm \nu_I)^2 + (e^2qQ/4h)^2(3+\eta^2)]^{1/2} \quad (3)$$

where a is the hyperfine coupling for the given orientation of the paramagnetic species. The typical manifestations of HYSCORE spectra of $S = 1/2$, $I = 1$ systems have been discussed by Dikanov et al. [15].

2.4. Data handling and simulations

The CW EPR spectra were simulated using the Easyspin package, developed at ETH, Zurich (http://www.esr.ethz.ch). The time traces of the HYSCORE spectra were baseline-corrected with a third-order polynomial, apodized with a Hamming window and zero-filled. After 2D Fourier transformation, the absolute-value spectra were calculated and the HYSCORE spectra measured with different τ values were added. The HYSCORE spectra were simulated using the TRYSCORE program [16].

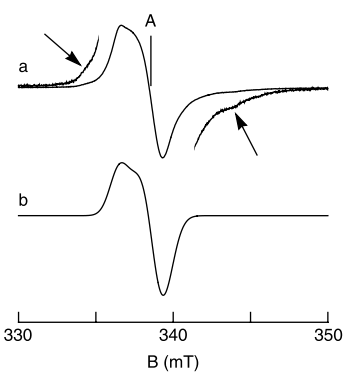

Fig. 1. (a): Experimental CW EPR spectrum of a frozen toluene solution of **2**, recorded at 140 K. The enlargements show the low- and high-field satellites due to the ^{47}Ti and ^{49}Ti hyperfine interaction. (b): Simulation of (a) with $g_\parallel = 2.0013$, $g_\perp = 1.9868$.

3. Results and discussion

3.1. Analysis of the CW EPR spectra

Fig. 1a shows the EPR spectrum of the uncharacterized titanium-containing catalyst precursor **2** in a frozen solution of toluene at 140 K. The EPR spectrum can be ascribed to an $S = 1/2$ system with an axial **g** tensor ($g_\parallel = 2.0013$, $g_\perp = 1.9868$; simulation in Fig. 1b). The g values are similar to those observed for other Ti(III) complexes ($3d^1$ ground state) [5,6a,7a,10] and prove the presence of the Ti(III) oxidation state of the complex. The g values of **1** ($g_\parallel = 1.938$, $g_\perp = 1.986$) are also characteristic for Ti(III) complexes [8d,e,f], but are clearly different from those observed for **2**. Note that for **1**, $g_\parallel < g_\perp$, and for **2**, $g_\parallel > g_\perp$.

The g values depend strongly on the crystal field parameters. In a trigonal field, Ti(III) in octahedral coordination generally yields an EPR spectrum with $g_\parallel > g_\perp$ [17]. We will further address this situation as *case 1*. A clear example is given by the hydrated Ti(III) ion in a frozen 2-propanol–water mixture [17b]. The complex has D_{3d} symmetry with the unpaired electron residing mainly in the d_{z^2} orbital and it is characterized by $g_\parallel = 1.994$, $g_\perp = 1.896$.

For Ti(III) in a tetrahedral crystal field with tetragonal compression (unpaired electron in the d_{z^2} orbital) (*case 2*), the g values calculated to first order are given by [18]

$$g_\parallel \approx g_e \text{ and } g_\perp \approx g_e - 6\lambda/\Delta \quad (g_\parallel \approx 2.0023 > g_\perp) \quad (4)$$

whereas the g values of Ti(III) in a tetrahedral field with tetragonal elongation (unpaired electron in the $d_{x^2-y^2}$ orbital) (*case* 3) are

$$g_\parallel \approx g_e - 8\lambda/\Delta \text{ and } g_\perp \approx g_e - 2\lambda/\Delta \quad (g_\parallel < g_\perp) \quad (5)$$

where the spin–orbit coupling constant $\lambda = 154$ cm^{-1} and Δ is the tetrahedral splitting parameter. On the other hand, for Ti(III) in an octahedral field with tetragonal elongation (unpaired electron in the d_{xy} orbital) (*case 4*), the g values calculated to first order are [19]

$$g_\parallel \approx g_e - 8\lambda/\Delta \text{ and } g_\perp \approx g_e - 2\lambda/\delta \quad (6)$$

where Δ and δ are the octahedral and tetragonal splitting parameters, respectively.

The observed principal g values found for **2** are in agreement with *cases 1* and *2* (unpaired electron in the d_{z^2} orbital) and with *case 4* (unpaired electron in the d_{xy} orbital), provided that $4\delta < \Delta$. The principal g values of **1** agree with *case 3* (unpaired electron in the $d_{x^2-y^2}$ orbital) and *case 4* (unpaired electron in the d_{xy} orbital). It should also be noted that the g values observed for **1** are very similar to those found for various VO^{2+} complexes ($(d_{xy})^1$ ground state) [20]. For **1** and **2**, the actual situation may be more complicated than

described by Eqs. (4)–(6) due to the overall low symmetry of the complexes. Nevertheless, Eqs. (3)–(5) can be used as a basis for a semiquantitative assessment.

Weak satellites detectable on the high- and low-field side of the EPR spectrum (see enlargements in Fig. 1a) result from the hyperfine interactions of the unpaired electron with ^{47}Ti ($I = 5/2$, $g_n = -0.31484$) and with ^{49}Ti ($I = 7/2$, $g_n = -0.31491$). The hyperfine parameters could not be obtained because the signals are obscured completely by the intense spectrum of titanium with zero nuclear spin and because ^{47}Ti and ^{49}Ti have nearly the same g_n value.

3.2. Analysis of the HYSCORE spectra

Fig. 2a,c shows the HYSCORE spectrum of a frozen toluene solution of **2** taken at observer position A (Fig. 1). Contributions of three types of nuclei can be distinguished: ^{14}N, ^{6}Li/^{7}Li and ^{1}H.

3.2.1. Lithium interactions

In the (+, +) quadrant of the HYSCORE spectrum of **2** (Fig. 2a), two peaks appear at (ν_I, ν_I) where ν_I are the nuclear Zeeman frequencies of ^{6}Li and ^{7}Li. The intensity ratio of the two signals agrees with the natural abundance of the two lithium isotopes (7.5 and 92.5%). If we assume that the isotropic hyperfine coupling, a_{iso}, is negligible and the HYSCORE signals are mainly determined by the dipolar hyperfine interaction, the shape of the two peaks leads to an estimated distance r between the unpaired electron and the lithium nucleus of 0.42–0.65 nm (using Eq. (1)). Both LiCl and MeLi are used in the synthesis of **2**, which explains the presence of lithium signals in the HYSCORE spectrum. Attempts to remove all lithium from the sample were unsuccessful. However, since **2** showed clear catalytic activity at all times when a co-catalyst was added, we think that the presence of lithium does not compromise any further results in this work. On the contrary, the observation of the lithium signals shows the power of the HYSCORE method in identifying the surroundings of a paramagnetic compound, where other analytical methods failed.

3.2.2. Nitrogen interactions

The features observed in the (−, +) quadrant of the HYSCORE spectrum in Fig. 2a can be ascribed to the interaction with a nitrogen nucleus. The synthesis of **2** was designed as to coordinate an amine to the titanium ion. The observation of the nitrogen interaction indicates that this ligation has indeed taken place. Since the cross-peaks between the DQ frequencies, ν_α^{DQ} and ν_β^{DQ}, appear in the (−, +) quadrant, the hyperfine interaction with the nitrogen nucleus is larger than twice the nuclear Zeeman frequency. The shape of the observed DQ ridges (parallel to the antidiagonal) is indicative of a substantial anisotropy of the hyperfine interaction. Fig. 3 shows the HYSCORE spectrum of a frozen toluene solution of the known Ti(III) catalyst precursor, (η^5-$C_5Me_4SiMe_2N^tBu$)TiMe (**1**). The dominant signals observed in the HYSCORE spectrum of **1** stem from the interaction with the nitrogen nucleus of the silylamido ligand. A comparison of Fig. 2a and Fig. 3 reveals that the nitrogen interactions observed in **1** and **2** are similar, but not identical. The difference between the two spectra in the [0–2, 0–2] MHz region may result from the base-line correction and does not reflect physical differences. From Eq. (3) and the position of the DQ cross-peaks, it can be derived that the main difference between the two observed nitrogen interactions is caused by the nuclear quadrupole interactions. For the ^{14}N nucleus coordinated to Ti^{3+} in **2**, $(e^2qQ/4h)^2(3+\eta^2) = 0.61$ MHz^2, and in **1** $(e^2qQ/4h)^2(3+\eta^2) = 1.26$ MHz^2. Since $0 \le \eta \le 1$, we find $1.56\ \text{MHz} \le |e^2qQ/h| \le 1.80$ MHz for **2** and $2.25\ \text{MHz} \le |e^2qQ/h| \le 2.59$ MHz for **1**. In order to get more precise values of these parameters, simulations of the HYSCORE spectra were undertaken using TRYSCORE [16], whereby not only the shape of the DQ peaks was optimized, but also the positions of the cross-peaks between the different single-quantum (SQ) frequencies and of the SQ–DQ cross-peaks were fitted (see arrows in Figs. 2a and 3). The best-fit parameters for the nitrogen hyperfine and nuclear quadrupole interaction observed for **1** and **2** are given in Table 1. To our knowledge, this is the first time that hyperfine and nuclear quadrupole data of titanium-bound nitrogens are reported. The small **g** anisotropy (and the consequently poor orientation selectivity) rendered the determination of the full set of parameters difficult; hence, the errors on the simulation parameters are relatively large. Fig. 2b shows the simulation of the ^{14}N part of the HYSCORE spectrum in Fig. 2a. Taking into account that the simulation was done under the assumption of ideal pulses and that the TRYSCORE simulation program involves a number of simplifications over the general theoretical model [16], the agreement with the experiment is satisfactory.

Based on the g values of **2**, the unpaired electron can possibly reside either in the d_{xy} or the d_{z^2} orbital, whereas the g values of **1** predict that the unpaired electron resides in the d_{xy} or the $d_{x^2-y^2}$ orbital. In the following discussion, we therefore compare the observed nitrogen couplings with those reported for transition metal complexes with the unpaired electron in one of these three d-orbitals.

The observed isotropic hyperfine couplings, $|a_{iso}|$, are comparable to those found for nitrogens bound to an oxovanadium cation, VO^{2+} [21–29]. The reported VO^{2+} complexes are characterized by a d^1 ground state with the unpaired electron in the d_{xy} orbital. In the VO^{2+} complexes, the nitrogen hyperfine principal val-

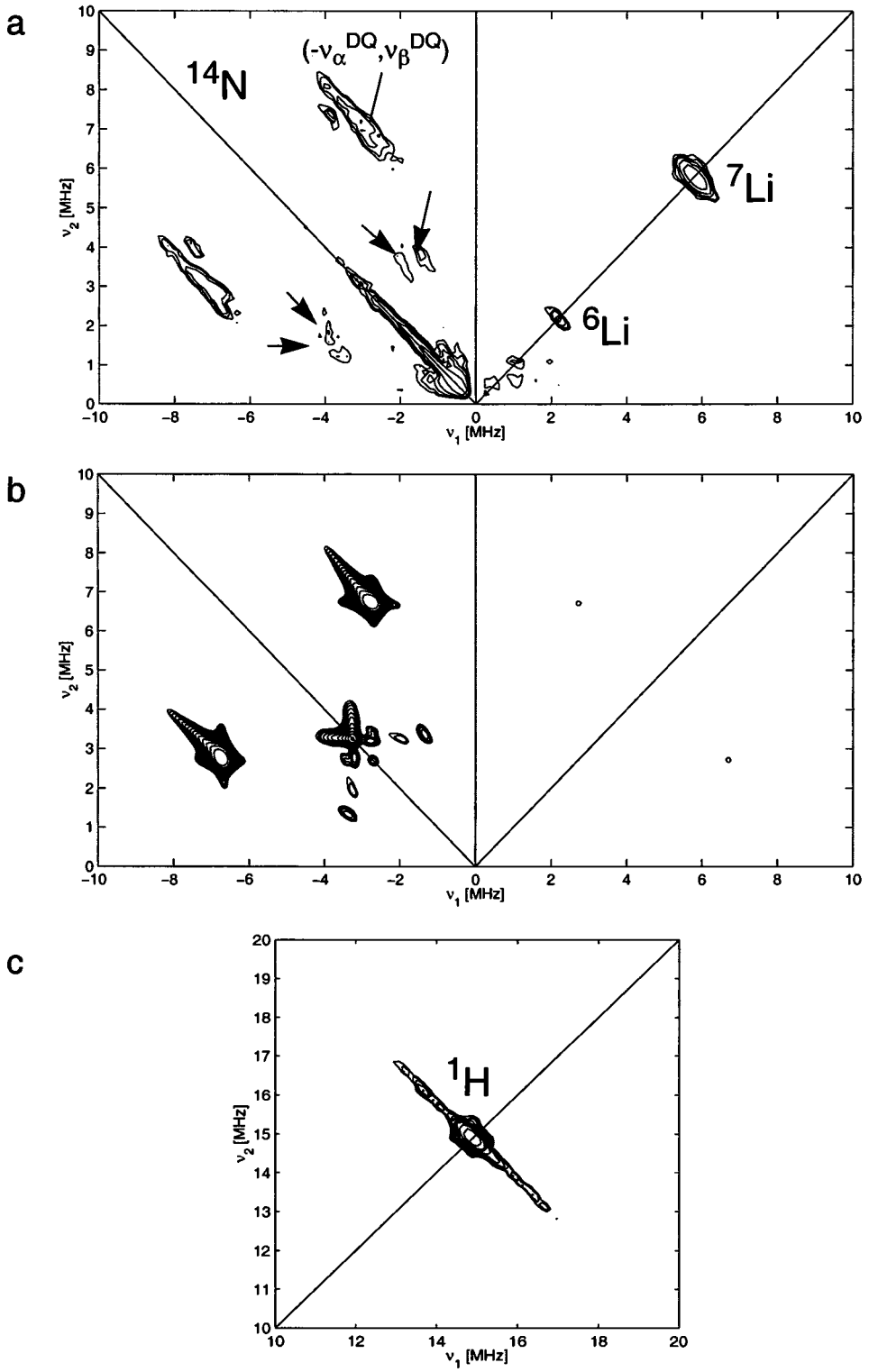

Fig. 2. HYSCORE spectra of a frozen toluene solution of **2**, taken at observer position A (Fig. 1a). (a): Experimental nitrogen and lithium HYSCORE spectrum. The arrows indicate the cross-peaks involving the nitrogen single-quantum frequencies. (b): Simulation of the nitrogen spectrum in (a). (c): Experimental proton HYSCORE spectrum.

ues are negative. This can be understood in terms of an indirect spin transfer mechanism, where the nitrogen orbital is polarized by an exchange interaction with the unpaired electron on the vanadium d-orbital [29]. Since the β electron spin in the nitrogen lone-pair receives more Coulomb repulsion from the unpaired α electron

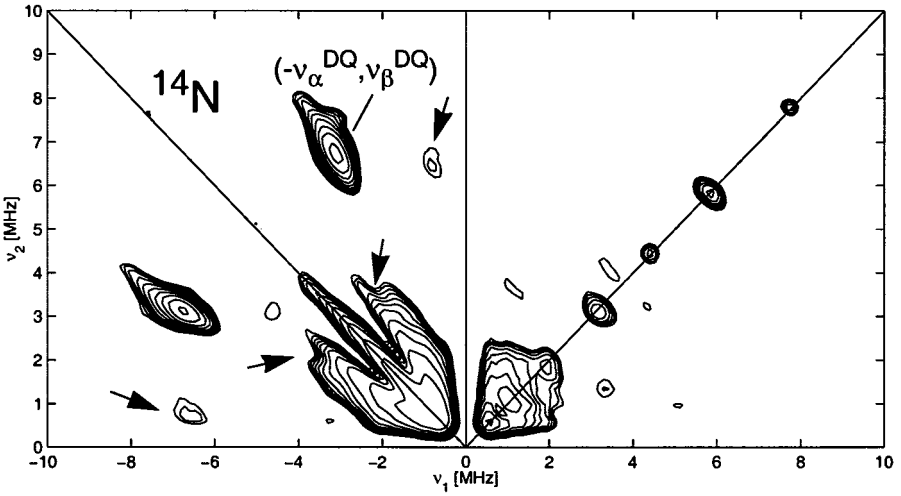

Fig. 3. Experimental HYSCORE spectrum of a frozen toluene solution of **1**, taken at an observer position corresponding to $g_{\perp}$. The arrows indicate the cross-peaks involving the nitrogen single-quantum frequencies.

spin on the vanadium, a negative spin density will be induced in the lone-pair orbital. If the VO^{2+} and Ti(III) complexes have similar ground states, the nitrogen hyperfine interactions observed for **1** and **2** are expected to be negative. ESEEM and ENDOR studies of ^{14}N nuclei directly coordinated to VO^{2+} have shown that there exists a useful correlation between the magnitude of a_{iso} and the type of nitrogen [21,23]. $|a_{iso}|$ is found to be ca. 4–5 MHz for sp^3-hybrid amine nitrogens [21,22], 6–7 MHz for sp^2-hybrid nitrogens [21–28] and ca. 7.5 MHz for sp-hybrid isothiocyanate nitrogens [21]. Although more complexes should be measured in order to establish whether this trend is also applicable to Ti(III) compounds, it is interesting to note that $|a_{iso}| = 4.4$ and 4.81 MHz for the sp^3 nitrogens of **1** and **2**, respectively.

On the other hand, the isotropic nitrogen hyperfine couplings observed in this study are also in the same order of magnitude albeit 1.5 to 2 times higher than those reported for the nitrogens bound to Co^{2+} ions [30–32]. Five-fold coordinated low-spin Co(II) complexes are characterized by a d^7 ground state where the unpaired electron resides in the d_{z^2} orbital. Consequently, based on the nitrogen couplings a $(d_{z^2})^1$ ground state cannot be excluded for **2** at this point.

Finally, the isotropic hyperfine couplings observed for nitrogens coordinated to Cu^{2+} ions (d^9 ground state with the unpaired electron in the $d_{x^2-y^2}$ orbital) [33] are an order of magnitude larger than those found in **1**. This seems to exclude the possibility of a $(d_{x^2-y^2})^1$ ground state for **1**. This also agrees with the observed similarity between the principal g values of **1** and those observed for the VO^{2+} complexes [20].

The difference in the nuclear quadrupole couplings between **1** and **2** is interesting. At first sight, one would ascribe the difference to the fact that in **1** the nitrogen is bound to Si, whereas it is carbon-bound in **2**. However, nuclear quadrupole resonance studies on free silyl and alkyl amines have shown that the difference in $|e^2qQ/h|$ is only 7% and the value is largest for the alkyl nitrogens [34]. The main difference in the observed nuclear quadrupole values must thus stem from the fact that the nitrogen in **1** is three-fold coordinated, whereas the nitrogen in **2** is expected to be four-fold coordinated (amide coordinating to Ti(III)). Similarly, studies of VO^{2+} complexes already showed a dependence of the $|e^2qQ/h|$ values of the ligand nitrogens on their hybridization type [21]. This opens the possibility to use the nitrogen nuclear quadrupole interactions to identify binding types in Ti(III) complexes.

Furthermore, the nitrogen hyperfine interaction in **1** is found to be more anisotropic than the one in **2**. This might be related to a difference in the Ti–N distance for the complexes **1** and **2**.

The above analysis shows that HYSCORE can be used to *determine ligation of amino nitrogens* in Ti(III)

Table 1
Principal values of the hyperfine matrices and nuclear quadrupole interactions of the ligand nitrogen of **1** and **2**, derived from X-band HYSCORE spectra

	1	**2**
$\|A_x\|$, $\|A_y\|$, $\|A_z\|$ (MHz) (± 0.2 MHz)	3.5, 3.5, 6.2	4.2, 4.2, 6.2
$\|a_{iso}\|$ (MHz)	4.4	4.87
α_A, β_A, γ_A (°) ($\pm 20°$)	0, 90, 0	0, 100, 0
$\|e^2qQ/h\|$ (MHz) (± 0.1 MHz)	2.3	1.6
η (± 0.1)	0.9	0.9
α_Q, β_Q, γ_Q (°) ($\pm 20°$)	90, 90, 0	100, 100, 0

The directions (Euler angles) of the hyperfine matrices and nuclear quadrupole tensors with respect to the **g** principal directions are also given.

complexes. Although at present there is not yet sufficient knowledge on the hyperfine and nuclear quadrupole data of different titanium-bound nitrogens, the HYSCORE method furthermore has a potential of becoming an important tool to *identify the nitrogen binding types* in Ti(III) catalytic compounds in frozen solution, when data about more such systems will be available.

3.2.3. Proton interactions

Fig. 2c shows the proton HYSCORE spectrum of **2**. The majority of the protons in the compound interact weakly with the unpaired electron (hyperfine coupling < 1 MHz), whereas one type of protons interacts more strongly with the unpaired electron (maximum hyperfine interaction ~ 4.2 MHz). The proton HYSCORE spectrum of **1** (not shown) looks very similar, with the largest observed proton coupling amounting to 5.4 MHz. A CW ENDOR study of $[(\eta^5\text{-}CH_3C_5H_4)Ti(\eta^8\text{-}C_8H_8)]$ revealed that the hyperfine values of the methyl protons in the cyclopentadienyl ring lie between 0.7 and 0.9 MHz [10b], so that the methyl protons of the Cp* ligand are expected to contribute only to the central peak in the HYSCORE spectra of **1** and **2** (hyperfine interactions smaller than 1 MHz). The larger hyperfine coupling observed for **1** can most probably be ascribed to the protons of the directly coordinating methyl group. The fact that the HYSCORE spectra of **2** show proton hyperfine splittings up to 4.2 MHz indicates that a similar direct ligation of an alkyl group is taking place. In **2**, Ti(III) is indeed expected to ligate to two methyl groups. Although a full analysis of the proton interactions is beyond the scope of the present work, we will summarize how one can proceed from this point onwards in cases where a full identification of the titanium ligands is needed. In order to verify the above-mentioned assumptions on the proton couplings, **1** and **2** should be synthesized using selectively deuterated educts. For example, the synthesis and measurement of $(\eta^5\text{-}C_5Me_4SiMe_2N^tBu)TiCD_3$ will directly elucidate the origin of the 5.4 MHz coupling. Furthermore, the use of deuterated solvents can help to track down a possible solvent ligation to the Ti^{3+} ion. Solvent ligation has already been observed for $(Cp_2TiCl)_2ZnCl_2$–THF and could be detected by the combination of CW ENDOR and solvent deuteration [10a].

4. Conclusions

In this work, both the Ti(III) catalyst precursors $(C_5Me_4(CH_2)2NMe_2)TiMe_2$ and $(\eta^5\text{-}C_5Me_4SiMe_2\text{-}N^tBu)TiMe$ were studied using CW and pulse EPR. For the former catalyst component no NMR or X-ray data are available. The observation of the characteristic CW EPR spectrum proves that at least part of this monocyclopentadienyl compound is in the Ti(III) form. Using HYSCORE, the ligation of nitrogen to the Ti^{3+} ion can be confirmed. Comparison of the hyperfine couplings of the new Ti(III) complex with those found for the amide nitrogen in $(\eta^5\text{-}C_5Me_4SiMe_2N^tBu)TiMe$, shows that HYSCORE forms a promising tool to evaluate the Ti–N bonds in different Ti(III) catalysts. Furthermore, the observation of different types of proton interactions opens the way to use selective deuteration of the educts to track down the different ligands surrounding the metal ion in uncharacterized Ti(III) catalysts. Finally, the detection of lithium signals in the HYSCORE spectrum of **2** shows how sensitive the method is in observing the environment of the titanium nucleus.

This study demonstrates that HYSCORE spectroscopy has a potential of becoming a useful tool in the characterization of Ti(III) and other paramagnetic catalysts.

References

[1] For recent reviews see: (a) H.H. Brintzinger, D. Fischer, R. Mülhaupt, B. Rieger, R. Waymouth, Angew. Chem. Int. Ed. Engl. 34 (1995) 1143;
(b) M. Bochmann, J. Chem. Soc. Dalton Trans. (1996) 255;
(c) W. Kaminsky, M. Arndt, Adv. Polym. Sci. 127 (1997) 143;
(d) P.C. Möhring, N.J. Coville, J. Organomet. Chem. 479 (1994) 1.

[2] (a) J. Langmaier, Z. Samec, V. Varga, M. Horácek, K. Mach, J. Organomet. Chem. 579 (1999) 348;
(b) L. Jia, X. Yang, C.L. Stern, T.J. Marks, Organometallics 16 (1997) 842.

[3] (a) J.C. Flores, J.S. Wood, J.C.W. Chien, M.D. Rausch, Organometallics 13 (1994) 4140;
(b) J.C. Flores, J.S. Wood, J.C.W. Chien, M.D. Rausch, Organometallics 15 (1996) 4944;
(c) A. Grassi, A. Zambelli, F. Laschi, Organometallics 15 (1996) 480;
(d) Y.-X. Chen, P.-F. Fu, C.L. Stern, T.J. Marks, Organometallics 16 (1997) 5958.

[4] (a) R.K. Rosen, P.N. Nickias, D.D. Devore, J.C. Stevens, F.J. Timmers, US Patent 5374696, 1994;
(b) J.C. Stevens, F.J Timmers, G.F. Schmidt, P.N. Nickias, R.K. Rosen, G.W. Knight, S. Lai, European Patent 0416815A2, 1991;
(c) J.C. Flores, J.C.W. Chien, M.D. Rausch, Organometallics 13 (1994) 4140;
(d) H.G. Alt, K. Föttinger, W. Milius, J. Organomet. Chem. 572 (1999) 21;
(e) M. Galan-Feres, T. Koch, E. Hey-Hawkins, M.S. Eisen, J. Organomet. Chem. 580 (1999) 145;
(f) J.A. van Beek, G.H. van Doremaele, G.J. Gruter, G.H. Eggels, European Patent 0789718B1, 1998;
(g) J.A. van Beek, G.J. Gruter, European Patent 0805142A1, 1997;
(h) J.A. van Beek, G.J. Gruter, European Patent 0805142B1, 1999.

[5] T. Koch, S. Blaurock, F.B. Somoza, A. Voigt, R. Kirmse, E. Hey-Hawkins, Organometallics 19 (2000) 2556.

[6] (a) E. Samuel, F. Labauze, D. Vivien, J. Chem. Soc. Dalton Trans. (1979) 956;
(b) D. Gourier, D. Vivien, E. Samuel, J. Am. Chem. Soc. 107 (1987) 7418.
[7] (a) M. Horáček, V. Kupfer, U. Thewalt, M. Polášek, K. Mach, J. Organomet. Chem. 579 (1999) 126;
(b) G. Xu, E. Ruckenstein, J. Polym. Sci. A 37 (1999) 2481;
(c) J.C.W. Chien, Y. Salajka, S. Dong, Macromolecules 25 (1992) 3199;
(d) S.W. Ewart, M.J. Sarsfield, D. Jeremic, T.L. Tremblay, E.F. Williams, M.C. Baird, Organometallics 17 (1998) 1502.
[8] (a) A. Tuel, J. Diab, P. Gelin, M. Dufaux, J.-F. Dutel, Y.B. Taarit, J. Mol. Catal. 63 (1990) 95;
(b) Y. Wang, C. Yeh, J. Chem. Soc. Faraday Trans. 87 (1991) 345;
(c) A.M. Prakash, V. Kurshev, L. Kevan, J. Phys. Chem. B 101 (1997) 9794;
(d) A.M. Prakash, H.M. Sung-Suh, L. Kevan, J. Phys. Chem. B 102 (1998) 857;
(e) A.M. Prakash, L. Kevan, J. Catal. 178 (1998) 5862;
(f) A.M. Prakash, L. Kevan, M.H. Yahedi-Niaki, J. Phys. Chem. B 103 (1999) 831.
[9] (a) A. Schweiger, Angew. Chem. Int. Ed. Engl. 30 (1991) 265;
(b) C. Gemperle, A. Schweiger, Chem. Rev. 91 (1991) 1481;
(c) Y. Deligiannakis, M. Louloudi, N. Hadjiliadis, Coord. Chem. Rev. 204 (2000) 1;
(d) S. Van Doorslaer, A. Schweiger, Naturwissenschaften 87 (2000) 245;
(e) A. Schweiger, G. Jeschke, Principles of Electron Paramagnetic Resonance, Oxford University Press, Oxford, 2001.
[10] (a) G. Labauye, J.B. Raynor, E. Samuel, J. Chem. Soc. Dalton Trans. (1980) 2425;
(b) D. Gourier, E. Samuel, J. Am. Chem. Soc. 109 (1987) 4571.
[11] P. Höfer, A. Grupp, H. Nebenführ, M. Mehring, Chem. Phys. Lett. 132 (1986) 279.
[12] A. Pöppl, L. Kevan, J. Phys. Chem. 100 (1996) 3387.
[13] S.A. Dikanov, M.K. Bowman, J. Magn. Reson. A 116 (1995) 125.
[14] S.A. Dikanov, Yu.D. Tsvetkov, M.K. Bowman, A.V. Astashkin, Chem. Phys. Lett. 90 (1982) 149.
[15] S.A. Dikanov, L. Xun, A.B. Karpiel, A.M. Tyryshkin, M.K. Bowman, J. Am. Chem. Soc. 118 (1996) 8408.
[16] R. Szosenfogel, D. Goldfarb, Mol. Phys. 95 (1998) 1295.
[17] (a) H.M. Gladney, J.D. Swalen, J. Chem. Phys. 42 (1965) 1999;
(b) H. Tachikaw, T. Ichikawa, H. Yoshida, J. Am. Chem. Soc. 112 (1990) 977.
[18] J.A. Weil, J.R. Bolton, J.E. Wertz, Electron Paramagnetic Resonance: Elementary Theory and Practical Applications, chap. 8, Wiley, New York, 1994, pp. 213–238.
[19] J.R. Pilbrow, Transition Ion Electron Paramagnetic Resonance, chap. 3, Clarendon Press, Oxford, 1990, pp. 116–119.
[20] S.K. Misra, in: C.P. Poole, H.A. Farach (Eds.), Handbook of Electron Spin Resonance, vol. 2, Springer Verlag, New York, 1999, pp. 156–165.
[21] K. Fukui, H. Ohya-Nishigchi, H. Kamada, Inorg. Chem. 36 (1997) 5518.
[22] C. Buy, T. Matsui, S. Andrianambinintsoa, C. Sigalat, G. Girault, J.-L. Zimmermann, Biochemistry 35 (1996) 14281.
[23] K. Fukui, H. Ohya-Nishigchi, H. Kamada, M. Iwaizumi, Y. Xu, Bull. Chem. Soc. Jpn. 71 (1998) 2787.
[24] S.A. Dikanov, A.M. Tyryshkin, J. Hüttermann, R. Bogumil, H. Witzel, J. Am. Chem. Soc. 117 (1995) 4976.
[25] S.A. Dikanov, R.I. Samoilova, J.A. Smieja, M.K. Bowman, J. Am. Chem. Soc. 117 (1995) 10579.
[26] C.F. Mulks, B. Kirste, H. van Willigen, M.K. Bowman, J. Am. Chem. Soc. 104 (1982) 5906.
[27] E.J. Reijerse, J. Shane, E. de Boer, P. Höfer, D. Collison, in: N.D. Yordanov (Ed.), Electron Magnetic Resonance of Disordered Systems, World Scientific, Singapore, 1991.
[28] B. Kirste, H. van Willigen, J. Phys. Chem. 86 (1982) 2743.
[29] C.P. Scholes, K.M. Falkowski, S. Chen, J. Bank, J. Am. Chem. Soc. 108 (1986) 1660.
[30] M.D. Wirt, C.J. Bender, J. Peisach, Inorg. Chem. 34 (1995) 1663.
[31] S. Van Doorslaer, R. Bachmann, A. Schweiger, J. Phys. Chem. A 103 (1999) 5446.
[32] S. Van Doorslaer, A. Schweiger, Phys. Chem. Chem. Phys. 3 (2001) 159.
[33] (a) T. Szabó-Plánka, G. Peintler, A. Rockenbauer, M. Gyõr, M. Varga-Fábián, L. Institórisz, L. Balázspiri, J. Chem. Soc. Dalton Trans. (1989) 1925;
(b) H.L. Van Camp, R.H. Sands, J.A. Fee, J. Chem. Phys. 75 (1981) 2098;
(c) S.P. Greiner, D.L. Rowlands, R.W. Kreilick, J. Phys. Chem. 96 (1992) 9132;
(d) T.G. Brown, B.M. Hoffman, Mol. Phys. 39 (1980) 1073.
[34] E. Schempp, M. Chao, J. Phys. Chem. 80 (1976) 193.